Limitations of Ignition Theory for Transient Exposure. Ignition of Solids Exposed to Radiation from a Compartment Fire

Santamaria S.*, Hadden R.M.[1]

The University of Edinburgh, School of Engineering, Edinburgh, UK
[*]Corresponding author's email: S.Santamaria-Garcia@ed.ac.uk

ABSTRACT

The piloted ignition of thermoplastic polymers exposed to transient irradiation is investigated. Previous research measured the radiation emitted through a full-scale, post-flashover compartment fire using Thin-Skin Calorimeters. This data is used in the present study to define the Incident Heat Flux time series to which the samples are exposed. Polymethyl-methacrylate and Polyamide 6 were used. A total of 20 experiments were performed in the Fire Propagation Apparatus. The temperature was recorded at depths of 4, 8, 12 and 16 mm from the surface. A regression analysis is used to estimate the temperature profile at each time step. The Net Heat Flux absorbed by the sample at the surface was calculated using Fourier's law. Conductive losses through the back face are also calculated. Assessing the evolution of the Net Heat Flux and the conductive losses, we found that under transient irradiation, there is a large uncertainty in the time to ignition of Polyamide samples as the surface phenomena introduces a non-negligible uncertainty which cannot be evaluated in current formulations. It was shown that surface phenomena affect mass transfer considerably, but has a lesser impact on the heat transfer process. An approach to study ignition based on controlling the absorbed energy is proposed for samples in which surface phenomena are significant.

KEYWORDS: Ignition, net heat flux, flammability.

INTRODUCTION

As the practice of fire safety engineering progresses towards a performance based design philosophy [1], it becomes ever more important to assess the definitions which underpin current design criteria. One such concept is the minimum separation between structures, which can be considered an extension of compartmentation. It is paramount to contain the fire to its room of origin and prevent any spread within the building or to nearby structures.

The current methodology used in the UK to assess the separation of buildings [2] establishes a minimum distance to the boundary of the property, as a function of the dimensions of the opening and the design fuel load. This is based on work conducted by Law [3]. The methodology allows an estimation of the Incident Heat Flux (IHF) as a function of distance. A key assumption behind the commonly used minimum distance tables found in standards is that the maximum irradiation permitted on a surface should not exceed 12.5 kW/m^2, considered as the critical IHF for the piloted ignition of wood. This is based on ignition studies where timber samples were exposed to constant irradiation.

The testing framework for analysing the flammability properties of a material [4-6], as well as the classical formulation of ignition theory [7], are built on the understanding that exposing materials to a constant IHF simplifies the experimental set-up and the mathematical expressions. However, what truly drives the ignition phenomenon is the net absorbed energy, which is a function of the boundary conditions (including the IHF) as well as the properties of the material.

Proceedings of the Ninth International Seminar on Fire and Explosion Hazards (ISFEH9), pp. 1078-1087
Edited by Snegirev A., Liu N.A., Tamanini F., Bradley D., Molkov V., and Chaumeix N.
Published by Saint-Petersburg Polytechnic University Press
ISBN: 978-5-7422-6498-9 DOI: 10.18720/spbpu/2/k19-123

The net flux of absorbed energy or Net Heat Flux (NHF) is not constant in a transient heating process. Even if the solid is exposed to a constant IHF, the NHF will decrease with time as the surface temperature and hence, the surface losses, increase. Different materials exposed to the same IHF will absorb different amounts of energy and this creates a fundamental difference in the way their flammability properties are assessed.

This paper studies the ignition of two different solids exposed to transient and constant IHF curves. The objective is to analyse the impact of a transient exposure by studying the NHF and assess the suitability of ignition theory, which is based on a constant exposure. The bench-scale experiments are informed by IHF curves measured from full-scale compartment fires. By looking at the evolution of the NHF, we aim at advancing our current framework for evaluating the fire risk associated to a material.

PRIOR RESEARCH

A set of five, full-scale compartment fires was carried out to study the impact of exposed combustible (timber) linings on compartment fire behaviour. The specific aim was to analyse if self-extinguishment of the exposed timber could be observed once the imposed fuel load had burnt out. The different experiments considered different configurations of exposed timber linings. Full details of this study can be found in [8, 9]. Approximately cubic compartments of dimensions 2.72 x 2.72 x 2.77 m^3 were used, with one opening of dimensions 1.84 x 0.76 m^2. Data from three experiments presented by Hadden et al. [8] are used here. These relate to the following configurations of exposed timber: back wall and sidewall (Alpha 2), ceiling and back wall (Beta 2) and ceiling, side wall and back wall (Gamma). All other surfaces are considered to be inert.

The radiation emitted from the opening and the plume was measured using Thin Skin Calorimeter (TSC) [10] towers. TSCs consist of an Inconel disc (ϕ = 10 mm and thickness = 2 mm) embedded into the surface of a vermiculite board (100 x 100 mm^2 x 25 mm). The temperature evolution of the Inconel disc is recorded. By solving the energy balance at the control volume of the metallic disc it is possible to calculate the Incident Heat Flux. A second thermocouple measures the gas phase temperature evolution close to the disc's surface. Surface convective losses are calculated assuming free convection from a vertical hot plate. The calibration factor is calculated as a function of the disc's temperature. TSCs are calibrated using a radiant panel against results obtained with a Schmidt-Boelter gauge.

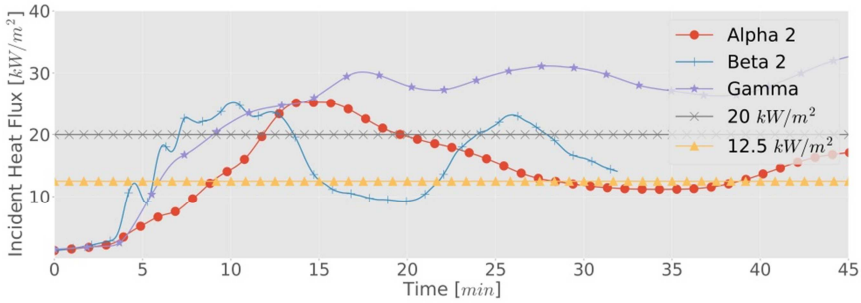

Fig. 1. Incident Heat Flux vs time for all experiments.

For this paper, we use IHF curves measured at 2 meters from the opening at a height of 1.6 meters, shown for Alpha 2, Beta 2 and Gamma in Fig. 1. The main difference between these curves is the oscillation defined by the growth/decay characteristic period of each test. All tests were terminated after 60 minutes. Figure 1 shows the IHF evolution for the first 45 minutes, as ignition testing is

limited to 30 minutes. Beta 2 presents the smallest characteristic time period, where the time between peaks is 18 minutes. Alpha 2 shows a longer period of oscillation, with a slightly lower rate of increase in the IHF after flashover. Gamma shows a similar rate of increase to Beta 2 but no oscillations are observed, as an approximate steady value of 30 kW/m^2 is maintained until end of testing.

After flashover (~ 5 min for all tests), all curves show a continuous increase in the IHF perceived by the TSCs. If we assume a linear increase (constant rate of change) between flashover and the maximum IHF, the rate of change of the irradiation perceived by the TSCs is approximately 28 – 42 W/m^{2}s. This is in agreement with the values used by Santamaria et al [11] when studying the ignition of PA6 samples exposed to linearly increasing IHF.

In addition to these, constant IHFs of 20 and 12.5 kW/m^2 were used for comparison. 12.5 kW/m^2 is the commonly used critical IHF for piloted ignition of timber. 20 kW/m^2 is above PA6's and PMMA's critical IHF (CHF). The critical IHF for PMMA is 10 kW/m2 and for PA6 is 15 kW/m^2 [12]. The CHF is only defined for constant irradiation.

EXPERIMENTAL METHODOLOGY

Ignition experiments were undertaken using the Fire Propagation Apparatus [5]. This allows the heat flux incident on a sample be rapidly changed according to the values described above which cannot be achieved with other apparatus.

Samples of Polymethyl-methacrylate (PMMA) and polyamide 6 (PA6) are exposed to the five different IHF time series. Both PMMA and PA6 are thermoplastic polymers and their ignition behaviour has been studied extensively under constant IHF [13, 14]. A reduced number of studies have investigated their ignition behaviour under transient irradiation [11, 15].Samples were of dimensions 85 x 85 x 25 mm and 85 x 85 x 20 mm for PMMA and PA6 respectively. Each combination of IHF time series and material were repeated once.

Aluminium foil and two layers of ceramic paper insulation wrap the side of the samples to limit heat and mass transfer in the direction perpendicular to the IHF. Four K-type thermocouples (ϕ = 1 mm) record in-depth temperature at intervals of 4, 8, 12 and 16 mm from the surface. The samples rests on an aluminium block, measuring 90x90x20 mm, where the additional dimensions ensure that the total sample plus the insulation rest on the block. A thermal conductive paste improves heat conduction between the sample's back face and the aluminium block, and so the thermal conductive resistance is neglected. The temperature increase in the Al block is also recorded with the same type of thermocouple. Table 1 shows the material properties used for PMMA, PA6 and the aluminium block. A similar diffusion of heat process is expected for both samples, given their similar thermal diffusivities, which permits an assessment on the impact of surface phenomena on ignition.

Table 1. Material properties

Material	Thermal conductivity: k, W/(m·K)	Density: ρ, kg/m^3	Specific heat capacity: c, J/(kg·K)	Thermal diffusivity: α, m^2/s
PMMA	0.27 [12]	1190*	2090 [12]	$1.09 \cdot 10^{-7}$
PA6	0.29*	1183*	1900 [12]	$1.29 \cdot 10^{-7}$
Aluminium	205*	2707 [12]	896 [12]	-

* Data provided by the manufacturer.

A pilot flame is used, located 10 mm from the edge of the sample and at a height of 10 mm from the surface. The IHF is calibrated at the start of each experimental period using a Schmidt-Boelter gauge and a quadratic regression is used to calculate the IHF as a function of the infrared lamp supply voltage, as shown in Equation 1.

$$IHF = c_0 + c_1 V + c_2 V^2 \tag{1}$$

It is assumed that:

- the heat transfer process is one dimensional,
- the solid behaves as inert until ignition,
- all material properties are invariant with temperature,
- the temperature at the back face of the sample (x = 25 mm for PMMA or x = 20 mm for PA6) is equal to the temperature of the aluminium block,
- the aluminium block behaves as a thermally thin solid and heat losses from it to the environment are negligible.

A regression analysis is used at each time step to evaluate the temperature distribution within the solid. This allows the evolution of the absorbed energy in the solid to be calculated. In order to do this an assessment of the surface temperature is required. This is calculated from fitting a function that describes the temperature as a function of distance from the heated surface. For an inert solid exposed to a constant IHF, this function is described by Eq. (2) [7]. Where, T_0 is the initial temperature, q the IHF, h_t the total heat transfer coefficient, x the distance from the surface, α the thermal diffusivity, k the thermal conductivity, ρ the density, c the specific heat capacity and t the time. The total heat transfer coefficient (h_t) is obtained by linearizing the radiative heat losses and adding the convective losses [7].

$$T(x,t) = T_0 + \frac{q}{h_t}\left[erfc\left(\frac{x}{\sqrt{4\alpha t}}\right) - e^{\frac{h_t x}{\sqrt{\alpha}\sqrt{k\rho c}} + \frac{h_t^2 t}{k\rho c}} \cdot erfc\left(\frac{h_t\sqrt{t}}{\sqrt{k\rho c}} + \frac{x}{\sqrt{4\alpha t}}\right)\right] \tag{2}$$

Figure 2 shows a graphical representation of Eq. (2). These curves are obtained for a PMMA sample, 20 mm thick, using the properties shown in Table 1. The figure on the left shows the penetration of the thermal wave into the solid as time progresses. The figure on the right shows the effect of the linearized heat transfer coefficient on the temperature profile at t = 200 s (~ t_{ig} for PMMA when exposed to 20 kW/m^2). The total heat transfer coefficient has a considerable effect on the surface temperature but not on the thermal wave penetration (as this is determined by the thermal diffusivity).

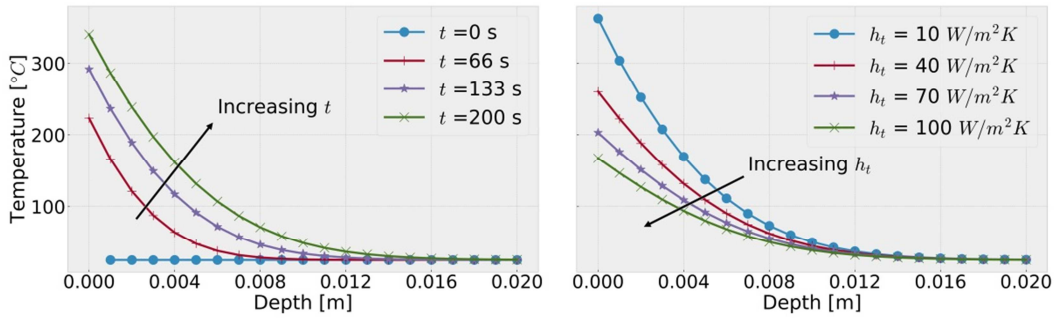

Fig. 2. Equation 2. Left: Temperature profile at different times (constant h_t). Right: Temperature profile at t = 200 s for different h_t. IHF = 20 kW/m^2 (constant).

The experimentally measured temperatures are fitted with an optimization process to determine the value of h_T by assessing the goodness of fit of Eq. (2) for all tests. The algorithm uses non-linear least squares to fit the Eq. (2) to the experimental data. The value of the heat transfer coefficient is constrained by the interval 0-60 W/(m^2·K). The initial guess at every time step was h_T = 20 W/(m^2·K). It is important to highlight that the heat transfer coefficient h_t is used as a fitting parameter. Therefore, it lumps uncertainties associated to the fitting of Eq. (2) to the experimental data and its value is chosen to minimize the fitting error. Therefore, this methodology is not expected to provide an accurate assessment of the heat transfer coefficient, but rather use h_t as the optimization parameter to ensure an adequate regression.

Equation (2) was derived for a solid exposed to constant irradiation. Hence, it does not completely capture thermal penetration for transient irradiation. This is addressed in the optimization for the heat transfer coefficient which indirectly accounts for the uncertainty introduced by the transient irradiation. At every time step a heat transfer coefficient is calculated which results in the best fit.

Figure 3 shows the results of the regression analysis at $t = t_{ig}$ for all tests on PMMA (only one of each repeated tests is shown for clarity). As expected, the regression provides a better fit for a constant irradiation. Although there is a systematic over prediction in the temperatures for the transient exposure scenarios, the trend is captured qualitatively and is used as a basis for the analysis that follows.

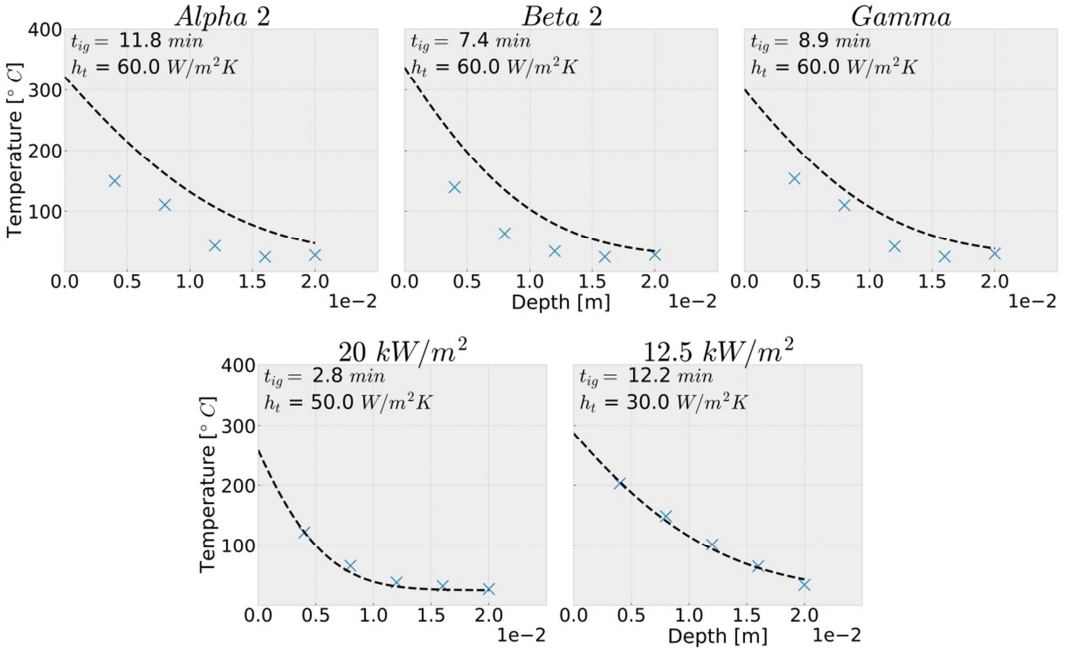

Fig. 3. Regression at $t = t_{ig}$. Fit was optimized for the heat transfer coefficient. Results shown for PMMA.

To obtain the NHF, Fourier's law is used with numerical differentiation for the rate of change of the temperature with depth, using a cell width of 0.5 mm, as shown in Eq. (4).

$$NHF = -k\frac{dT}{dx} \sim k\frac{T_{surf} - T_{0.5mm}}{0.0005} \tag{4}$$

A visual camera recorded all experiments and time to ignition is defined as the delay time between beginning of the exposure and the onset of flaming. Flashing before ignition did not occur in most

experiments, with the exception of Alpha 2 and Beta 2 exposures for PA6. The conductive losses to the aluminium block are calculated using Eq. (5), assuming negligible heat losses from the aluminium to the environment. A smoothing algorithm is used to reduce the noise given by the numerical differentiation of *dT*/*dt*.

$$Losses_{conductive} = mc_p \frac{dT}{dt} \sim mc_p \frac{\Delta T}{\Delta t} \tag{5}$$

RESULTS AND DISCUSSION

Table 2 shows a summary of the time to ignition and surface temperature (calculated) at ignition for all experiments. For the time to ignition, PMMA presents a small range of values whereas the scatter for PA6 results is considerable for transient and constant IHF. Furthermore, ignition was not attained when the samples were exposed to Alpha 2 or 12.5 kW/m^2. The latter was expected as the CHF for PA6 is 15 kW/m^2. For a constant IHF, the ignition temperature of PA6 is 432 – 497 ˚C and for PMMA 378 – 383 ˚C [12].

Table 2. Average time to ignition and surface temperature (calculated) at ignition. Values between brackets show maximum and minimum. NI refers to No Ignition. [max - min]

Material	Exposure	t_{ig}, min	T_{surf} , ˚C
	Alpha 2	11.9 [12.0–11.9]	327 [323–331]
	Beta 2	7.5 [7.5–7.5]	342 [339–344]
	Gamma	9.0 [9.0–8.9]	296 [301–291]
	20 kW/m^2	2.95 [2.8–3.1]	264 [260–268]
	12.5 kW/m^2	12.7 [12.6–12.8]	279 [289–269]
PA6	Alpha 2	- [NI–NI]	-
	Beta 2	[12.6–25.8]	355 [344–366]
	Gamma	15.3 [15–15.5]	453 [466–439]
	20 kW/m^2	13.5 [11.1–15.8]	342 [324–360]
	12.5 kW/m^2	> 25 [–]	-

Constant IHF

Figure 4 shows the NHF absorbed at the surface for samples exposed to constant IHF. The NHF is calculated from Eq. (4). This depends on the accuracy of the regression analysis used to define the temperature profile and, in particular the surface temperature. It is worth noting that the NHF, as calculated in this study, does not depend on the optical properties of PMMA or PA6. The temperature increase that is measured in the solid already reflects the effective absorbed energy by the sample. This is also valid for transient IHF. This assumes negligible in-depth absorption of radiation, observed for low, constant IHFs (< 60 kW/m^2) [16]. To the knowledge of the authors', in-depth absorption of radiation has not been studied under transient irradiation.

The trends of NHF are similar for both materials and characterised by an initial peak followed by a sharp decline and a long tail of low heat flux. Despite the similarity in shape, there is a considerable difference between the NHF and ignition times for the two materials. The absorbed energy will depend on the thermo-physical and optical properties of the tested material. The changes in material properties, affect the Biot and Fourier numbers which dominate the heat transfer processes. Surface phenomena can also impact energy absorption, as shown by Fig. 4, where the absorbed energy prior

to ignition varies between materials, and, for the two samples of PA6 exposed to 20 kW/m^2. This is due to changes to the geometry of the system and bubbling of molten PA6. These changes do not affect the NHF reported in Fig. 4 since the NHF is calculated from the curve fit.

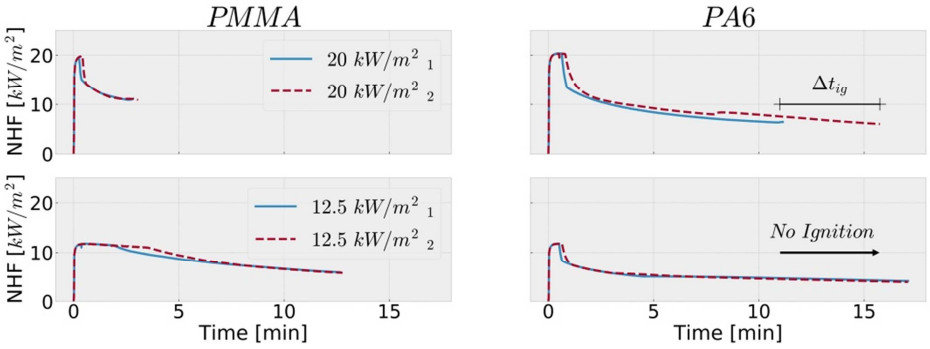

Fig. 4. Net Heat Flux for PMMA (left) and PA6 (right) exposed to constant IHF of 20 kW/m^2 (top row) and 12.5 kW/m^2 (bottom row).

Figure 5 shows the conductive losses through the back face as calculated by Eq. (5). For PMMA, the conductive losses remain lower than 10% of the IHF whereas, for PA6, this value increases to approximately 15%. This is due to the longer time to ignition allowing penetration of the thermal wave, indicating that the semi-infinite solution may no longer be a good approximation. Both in Fig. 4 (NHF) and Fig. 5 (Conductive Losses), the data seems to show the attainment of a quasi-steady situation where the rate of change with time becomes negligible. Since the temperature gradient in the sample at ignition is not negligible (Fig. 3), the constant NHF for a non-inert solid can be explained by the pyrolysis process as highlighted by Torero [17]. Surface temperature does not increase and the absorbed energy is used for pyrolysis. This suggests that this methodology is appropriate to study the energy balance leading to ignition.

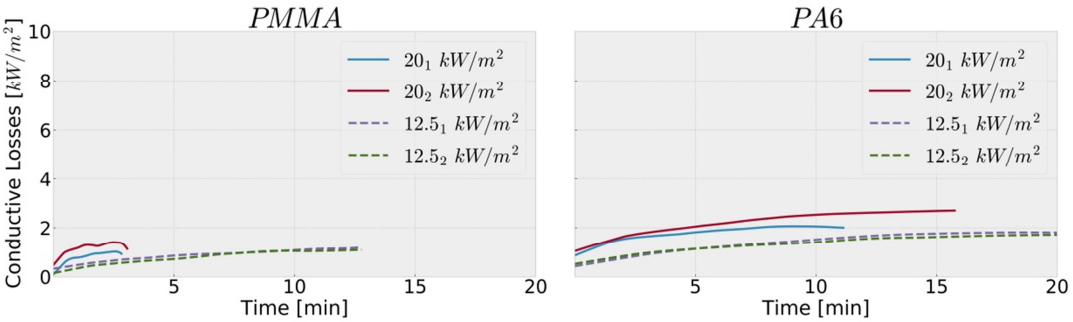

Fig. 5. Conductive losses to the aluminium block for constant exposures. Left: PMMA. Right: PA6. Solid lines show losses 20 kW/m^2 and dashed lines for 12.5 kW/m^2.

Transient IHF

Figure 6 shows the NHF absorbed at the surface by PMMA (solid lines) and PA6 (dashed lines). PMMA ignites at lower values of NHF for Alpha and Gamma exposures, compared to PA6. This agrees with PMMA having a lower CHF and ignition temperature. For Alpha 2 (left), ignition was not attained by PA6, even though the NHF is higher and the thermal properties of both materials are similar (Table 1). This difference can be explained by surface phenomena.

Figure 7 shows the pre-ignition behaviour of PA6 when exposed to Alpha 2. At 13 minutes, a maximum value of approximately 25 kW/m^2 for the IHF is reached, after which a slow decay follows. 20 minutes after the start of the exposure, the IHF has an approximate value of 20 kW/m^2, but a bubble has formed on the surface of the material, which prevents the free flow of pyrolyzates. If compared with Beta 2 and Gamma, the maximum NHF reached for Alpha 2 is lower. This phenomenon is not captured under constant heating rates and shows the importance of heating rate on the pyrolysis pathways.

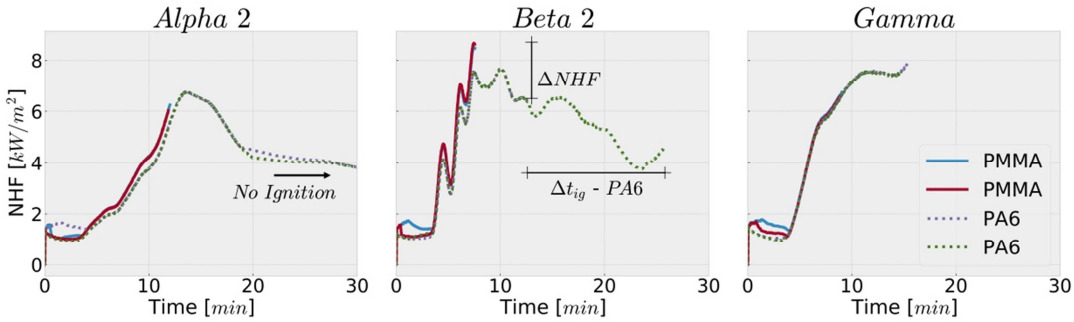

Fig. 6. Net Heat Flux for PMMA (solid lines) and PA6 (dashed lines) exposed to transient IHF.

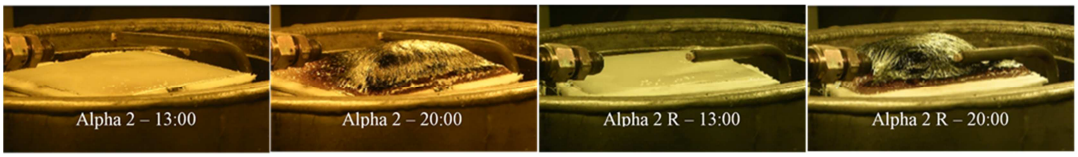

Fig. 7. Samples of PA6 exposed to Alpha 2. At 13:00, still shots show behaviour during the maximum IHF reached by the exposure. At 20:00, bubbling is shown, preventing ignition.

For PA6 samples exposed to Beta 2, there is a variability of approximately 100% in the time to ignition measured. Figure 8 shows images of both tests completed under this IHF curve. It is clear that surface phenomena taking place during the ignition of each sample (Fig. 8 left and right) differ. These differences can be explained by effects of the bubbling phenomena on the mass transfer process. This assessment implies that under the same exposure, small differences in boundary or initial conditions (mainly flow conditions) and material composition could result in considerable limitations when assessing the ignition behaviour of solids. Contrary to the other cases, PMMA ignites at a higher value of NHF, but at a lower total absorbed energy, since the time to ignition for PA6 is much longer.

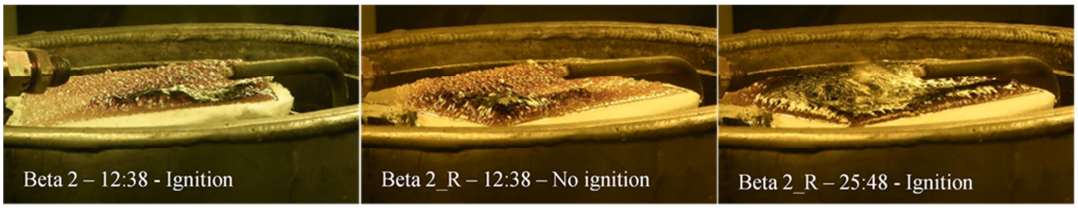

Fig. 8. Samples of PA6 exposed to Beta 2. Left: first experiment. Centre and right: repeat experiment.

Figure 9 shows the calculated conductive losses for both materials when exposed to transient IHF. The conductive losses remain approximately constant for all tests and between materials. Since the only difference between these experiments is the formation of the bubble, it can be inferred that the

bubble has a small effect on the heat transfer and the energy absorbed by the sample (and hence pyrolysis rate) and delays ignition simply be preventing mass transfer and the formation of a flammable mixture. Previous studies using linearly increasing IHF [11] have shown that the bubble effect will be reduced as the rate of change of the IHF increases.

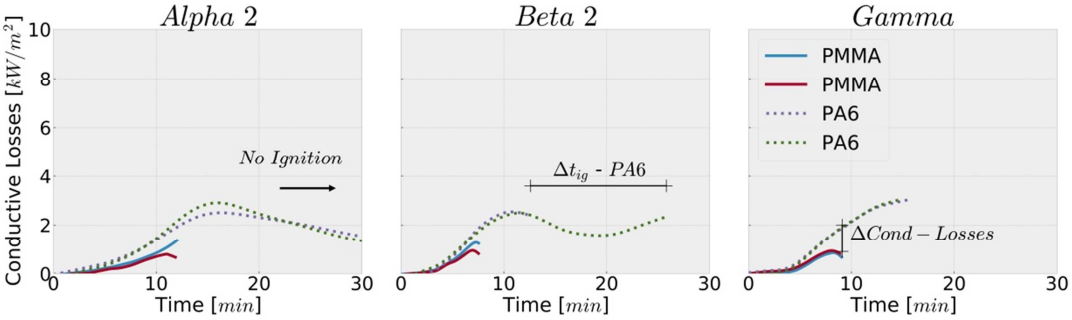

Fig. 9. Conductive losses for transient exposure for PMMA (solid lines) and PA6 (dashed lines).

CONCLUSIONS

This paper has investigated the effect of exposing samples of two different thermoplastic polymers to transient IHFs. The IHF curves were defined following measurements made from the radiation emitted by post-flashover compartment fires. The experiments analysed in this paper were completed using the Fire Propagation Apparatus. This study assessed the current ability for predicting ignition of these materials using ignition theory, traditionally derived for constant IHF.

The NHF's evolution was calculated for all tests. Even though PA6 and PMMA present similar thermos-physical properties, samples of the former reached ignition at higher values of the NHF, or even failed to ignite. This cannot be predicted using current ignition theory. Together with an assessment of the visual recordings, the processes driving ignition were investigated.

For samples exposed to a constant IHF, the NHF decreases with time, as the surface temperature and hence, the surface heat losses, increase. However, for samples exposed to increasing IHF, the NHF increases over time and so the ignition process differs as pyrolysis is driven by the NHF absorbed by the sample.

For transient exposures surface phenomena play a dominant and uncharacterized role. For PA6 samples, variations of up to 100% were measured in the ignition delay time. It is not currently possible to accurately manipulate surface phenomena during testing. This hinders our ability to understand their effects on ignition of materials exposed to transient irradiation.

Surface phenomenon was shown to have a considerable impact on ignition delay times through an effect on the mass transfer processes. The effect on heat transfer was shown to be small. This was evaluated through a comparison on the thermal diffusivities and an assessment of the conductive losses.

This study has shown that by exposing samples to transient IHF, different phenomena may dominate the ignition process. To accommodate for this complexities, it is proposed that new experimental frameworks are developed that seek to compare the ignition of materials by manipulating the flux of absorbed energy as opposed to the exposure.

ACKNOWLEDGEMENTS

Simon Santamaria is funded by the BRE Trust. Their support is gratefully acknowledged.

REFERENCES

[1] B.J. Meacham , R.L.P. Custer, Performance-Based Fire Safety Engineering: an Introduction of Basic Concepts, J. Fire Prot. Eng. 7(2) (1995) 35-53.

[2] 2010, T.B.R., Approved Document B, in Volume 2 - Buildings other than dwelling houses. 2007, HM Government: London.

[3] M. Law, Heat Radiation from Fires and Building Separation, D.o.S.a.I.R.a.F.O.C.J.F.R. Her Majesty's Stationery Office, London, p. 31, 1963.

[4] ISO 5660-1:2002, Reaction-to-fire tests – Heat release, smoke production and mass loss rate – Part 1: Heat release rate (cone calorimeter method), 2002.

[5] ASTM E2058–03, Standard Test Methods for Measurement of Material Flammability Using a Fire Propagation Apparatus (FPA), West Conshohocken, PA, 2013.

[6] ASTM E1321-13, Standard Test Method for Determining Material Ignition and Flame Spread Properties, ASTM International, West Conshohocken, 2013.

[7] J. Torero, Flaming ignition of solid fuels. SFPE Handbook of Fire Protection Engineering, 5th Ed., 2016 pp. 631-661.

[8] R.M. Hadden, A.I. Bartlett, J.P. Hidalgo, S. Santamaria, F. Wiesner, L.A. Bisby, S. Deeny, B. Lane, Effects of exposed cross laminated timber on compartment fire dynamics, Fire Saf. J. 91 (2017) 480-489.

[9] A.I. Bartlett, R.M. Hadden, J.P. Hidalgo, S. Santamaria, F. Wiesner, L.A. Bisby, S. Deeny, B. Lane, Auto-extinction of engineered timber: Application to compartment fires with exposed timber surfaces, Fire Saf. J. 91 (2017) 407-413.

[10] J.P. Hidalgo, C. Maluk, A. Cowlard, C. Abecassis-Empis, M. Krajcovica, J.L. Torero, A Thin Skin Calorimeter (TSC) for quantifying irradiation during large-scale fire testing, Int. J. Therm. Sci. 112 (2017) 383-394.

[11] S. Santamaria, R.M. Hadden, Experimental analysis of the pyrolysis of solids exposed to transient irradiaiton. Applications to ignition criteria, Proc. Combust. Inst. 37 (2018) 4221-4229.

[12] SFPE handbook of fire protection engineering, 2002, Quincy MA, NFPA.

[13] R.T. Long, J.L. Torero, J. Quintiere, A.C. Fernandez-Pello., Scale and Transport Considerations on Piloted Ignition of PMMA, In: Curtat, M. (Ed.), Fire Safety Science–Proceedings of the Sixth International Symposium, pp. 567-578, 2000.

[14] R. Carvel, et al., Determination of the flammability properties of polymeric materials: A novel method, Polym. Degrad. Stab. 96 (2011) 314-319.

[15] I. Vermesi, N. Roennera, P. Pironi, R.M. Hadden, G. Rein, Pyrolysis and ignition of a polymer by transient irradiation, Combust. Flame 163 (2016) 31-41.

[16] F. Jiang, J.L. de Ris, M.M. Khan, Absorption of thermal energy in PMMA by in-depth radiation, Fire Saf. J. 44 (2009) 106-112.

[17] J.L. Torero, Material properties that control ignition and spread of fire in micro-gravity environments, In: Proceedings of NHTC'00, ASME, Editor. 2000, ASME Heat Transfer Conference: Pittsburgh, Pennsylvania.